β-Decay and γ-Ray Spectroscopy with NaI Detectors

Jamison Lahman, Brandon Coleman, and Taylor Grueser

***Abstract*—Sodium-22 is an unstable isotope which decays through beta emission. In one instance, two 511 keV photons are emitted by positron annihilation in opposite directions to conserve momentum. In another instance, the an excited ^{22}Ne atom emits a single, 1275 keV photon with no angular correlation. Using two or more particle detectors simultaneously, we were able to distinguish an angle dependency. We were able to confirm a sharp angle dependency for the 511 photon keV emission and the coincidence rate was random within error for the 1275-511 rate. Additionally, materials absorbed photon energy differently depending on the energy of the ray and the attenuation coefficients. Placing various materials between our sample and detector, we were able to experimentally measure the attenuation coefficients for energies of 511 keV and 1275 keV. For Copper, we found values of 0.7445$\pm$0.0083cm^{-1} for a 551 keV photon and 0.4896$\pm$0.0077cm^{-1} for a 1275 keV photon. Both of these are within one standard deviation of the literature values. For Aluminium, we found values of 0.4053$\pm$0.0024cm^{-1} for a 551 keV photon and 0.1934$\pm$0.0055cm^{-1} for a 1275 keV photon, neither of which are in agreement with literature values.**

I. Introduction & Theory

Gamma rays are high energy photons which can be created during the decay process of radioactive elements such as ^{22}Na. In the same way a single electron, which is held in orbit by electromagnetic forces, releases a photon as it falls to a lower energy orbit, the nucleus of an atom can release a photon as it falls to a lower energy state. Since the atom is held together by the strong-nuclear force, the energy is much greater than for changes in electronic states.

A common apparatus for measuring photons is called a scintillator. A scintillator works by converting the ionization energy of photons into visible light which can then easily be collected. Most scintillators are inorganic crystals doped with activating material, similar to doping in semiconductors. In this experiment, a NaI(Tl), sodium-iodide doped with thallium was employed. NaI detectors are commonly used because of their cheap cost to make[1].

For ^{22}Na, a positron is emitted from the atom. In its positron annihilation, two photons are emitted with nearly identical energies. In order to preserve Newton's laws of motion, the momentum of the two must be equal and opposite.

$$\frac{dp_1}{dt} = -\frac{dp_2}{dt}. \tag{1}$$

Because of this conservation law, multiple detectors can be used to correlate a photon detection in one detector to an event in the other. The second photon emitted in the decay process in which the ^{22}Na decays to the first excited state of ^{22}Ne which produces one photon as it moves to the ground state and has no pair to conserve momentum and thus no angular correlation[2].

It is useful to know the mass attenuation coefficient, μ/ρ, when calculating the energy deposition by photons in materials. Different materials absorb the energy of photons at various rates. The rate of absorption is also dependent on the energy of the photon. The mass attenuation coefficient determines how well the material absorbes the energy of an incoming photon. The densities of materials are well known[3], so multiplying by the density gets the attenuation coefficient (usually in units of cm^{-1}) which appears in the following exponential relation:

$$\frac{I}{I_0} = e^{-\mu x}, \tag{2}$$

where I is the intensity and x is the length of the material traversed by the photon[1].

II. Experimental Details

Our experimental setup followed Figure 1. We had our NaI detector connected to a photo-multiplier which was powered by an external voltage supply. From there, the signal was amplified again and then sent to the multichannel analyzer and processed on a computer. To ensure we were receiving a signal from our set-up, we plugged an oscilloscope into the output of the the multichannel analyzer.

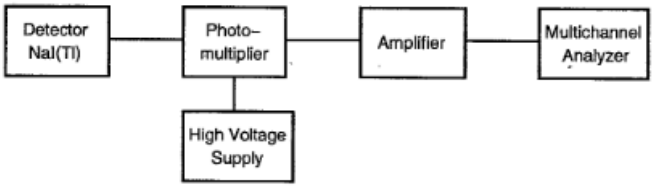

Fig. 1: A simplified rendition of the experimental apparatus used[1].

We had two detectors referred to as Gamma 1 and Gamma 2. Gamma 1 was a distance of 10.10$\pm$.05cm to the source while Gamma 2 was 10.30$\pm$.05cm. Gamma 1 is a type (7 D 4) detector while Gamma 2 is a type (6 D 4). Using the diagram in Figure 2, which describes the detectors used in the experiment, these correspond to diameters of 2.00 and 1.75 inches respectively. The diameter and the distance of the detector from the source both contribute to the solid angle, Ω. N_0 is simply the rate of emission from the sample. The detection rate of the detector, R, is given by the relation[2],

$$R = N_0 \frac{\Omega}{4\pi}. \tag{3}$$

Instructor: Paul King

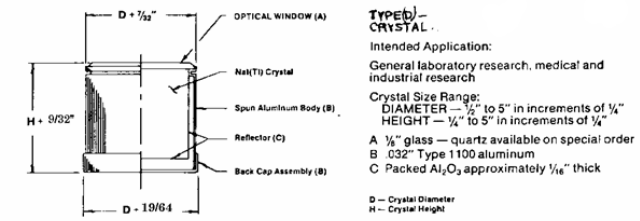

Fig. 2: Detector schematic for the NaI detectors[4].

Since Ω has an angle and radial dependency, the angle correlation will vary slightly with different radial components though this is will not be examined in this study. For example, a detector extremely close to a sample might not see any change with respect to a change in angle as the the radial component dominates in the solid angle calculation. The detectors are considered far enough from the sample to have adequate angle resolution while maintaining an adequate signal.

The gain of Gamma 1 was set to 450 while Gamma 2 was set to 266. For our gates, we set g_0 on the interval [160,290], g_1 on the interval [190,350], and g_2 on the interval [530,715].

For the attenuation coefficient calculations, aluminium and copper sheets were used. Each sheet had a thickness of 1.270±0.079cm

III. Data

To perform a rough energy calibration, we took data at 180° with no material obstructing the photon's paths at the beginning of each day for a total of six samples over three days. The peaks are roughly Poisson distributions so the error on of the mean is only dependent on the RMS of the peak and the number of counts, N[5]:

$$\sigma_{\bar{x}} = \frac{\sigma_x}{\sqrt{N}}. \tag{4}$$

The detectors are going to have energy calibrations which are independent of each other, so each must be calibrated separately. In all cases, the background was subtracted automatically using the program ROOT.

Data for Gamma 1 Energy Calibration

Bin Peak	Time (s)	Total Counts	RMS	$\sigma_{\bar{x}}$
285.1	600	34187	18.08	0.098
284.8	300	23817	17.75	0.12
284.7	600	49067	18.04	0.081
284.3	600	49095	18.06	0.082
359.8	450	1030	27.98	0.87
667.4	600	4586	26.95	0.098
666.5	300	3208	29.1	0.51
666.5	600	6605	28.32	0.35
666.0	600	6507	26.03	0.32

TABLE I: The 285 bin peak corresponds to the 511 keV photons from ^{22}Na while the 666 peak corresponds to the 1275 keV photons. The 360 peak is the 662 keV photon of decaying ^{137}Cs[6].

Data for Gamma 2 Energy Calibration

Bin Peak	Time (s)	Total Counts	RMS	$\sigma_{\bar{x}}$
259.5	600	19129	13.89	0.10
259.1	300	13174	14.30	0.12
254.9	600	24614	13.69	0.087
258.4	600	24864	13.80	0.088
328.1	450	604	16.33	0.66
612.9	600	2601	21.99	0.43
614.9	300	1767	21.00	0.50
609.2	600	3293	20.68	0.36
612.8	600	3300	21.36	0.37

TABLE II: The peak bin numbers corresponds to similar photon energies as Table I.

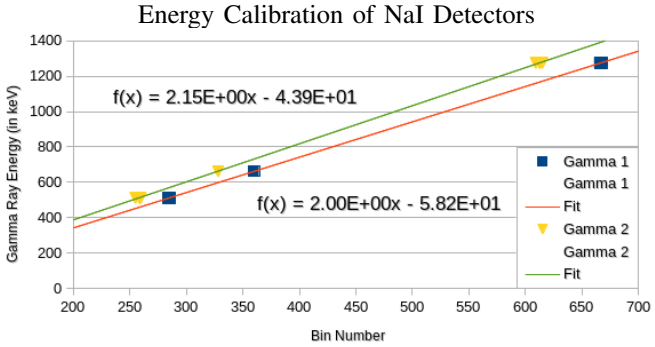

Fig. 3: A rough energy calibration the NaI detectors using decay peaks from ^{22}Na and ^{137}Cs. Data is taken from Tables I and II. The residuals are plotted in Figures 11 and 12.

Plotting the literature energy[6] as a function of the peak bin number yields Figure 3,

Performing a least-squares linear regression on the data in Figure 3 yields the following energy calibrations for Gamma 1 and Gamma 2 respectively:

$$y = (1.9995 \pm 0.0010)x - (58.22 \pm 0.32), \text{cov} = -3.1648\text{E-}4$$
$$y = (2.1535 \pm 0.0013)x - (43.90 \pm 0.36), \text{cov} = -4.3965\text{E-}4$$

To find the angle correlations, we simply integrate the number of similar incidences which occur simultaneously in both detectors while varying the angle between the detectors as seen in Figures 4, 5, and 6. Since the peaks are Poisson distributions, the error is simply[5]

$$\sigma_N = \sqrt{N}. \tag{5}$$

To find the attenuation coefficients for given materials, we measured the intensity of the peaks, i.e. the total number of counts after background subtraction, with various amount of thickness of material in between the source and the detectors.

Again the peaks are Poisson distributions so Eqn. (5) applies. Converting the errors to log-space, we find

$$\epsilon = \frac{\sigma_N}{I}. \tag{6}$$

Angle Correlation for Each Photon

Angle (°)	511-511	511-1275	1275-511	1275-1275
180.0	11145	42	34	0
175.0	8272	27	41	0
165.0	775	28	29	0
150.0	108	18	29	0
130.0	67	37	31	0
110.0	81	34	35	0
90.0	58	24	31	0

TABLE III: The angle measurements were taken in the anti-clockwise direction of Gamma 1 to Gamma 2. The first number represents which portion of the energy spectrum being recorded by Gamma 1 while the second number is similar for Gamma 2. The values indicate the number of coincidences detected in both detectors simulations.

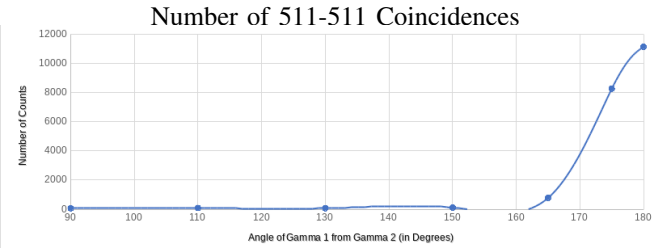

Fig. 4: The number of incidences in Gamma 1 which correspond to an event in Gamma 2 for the 511 keV photon regime as a function of angle between the detectors. The number of coincidences at each angle can help us determine whether or not the photons have an angle dependence between them.

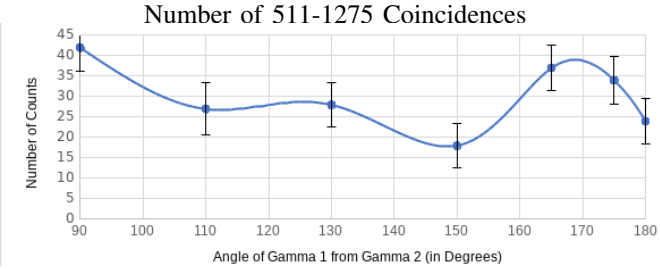

Fig. 5: The number of photons around the 511 keV photon incident in Gamma 1 which correspond to 1275 photon event in Gamma 2. The number of coincidences at each angle can help us determine whether or not the photons have an angle dependence between them.

IV. Results

Despite it being a rough energy calibration, we expected to see a constant relationship in between samples and days. As you can see by the residuals in Figures 11 and 12, the calibration is well outside of 5 standard deviations for numerous points. The calibration may be accurate, but it is by no means precise.

As seen by Figure 4, there is an obvious angular dependency for the 511 keV photons. The number of incidences around $\theta = 180°$ is far larger than any possible statistical fluctuation. The fluctuations in the coincidences in Figures 5 and 6 can be

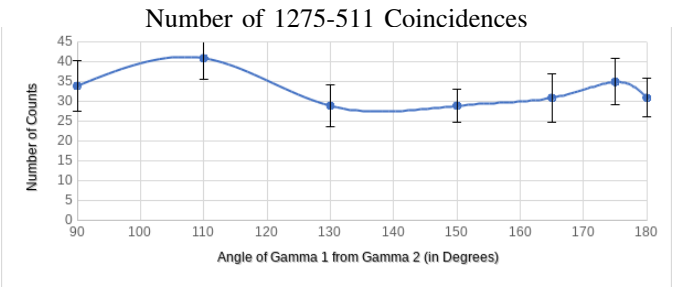

Fig. 6: The number of photons around the 1275 keV peak incident in Gamma 1 which correspond to 511 photon event in Gamma 2. The number of coincidences at each angle can help us determine whether or not the photons have an angle dependence between them.

Attenuation Through Copper for 511 keV Photon

Detector	Thickness (cm)	Intensity	$ln(I/I_0)$	ϵ
Gamma 1	0	47634	0	0.0032
	1.270	18336	-0.9547	0.0074
	2.540	6699	-1.962	0.012
	3.810	2742	-2.855	0.019
Gamma 2	0	26348	0	0.0043
	1.270	10587	-0.912	0.010
	2.540	4268	-1.820	0.018

TABLE IV: The intensity is simply the number of incidences detected by our detector. I_0 is the intensity with no material in between the source and detector. ϵ is the error in log-space as defined by Eqn. (6).

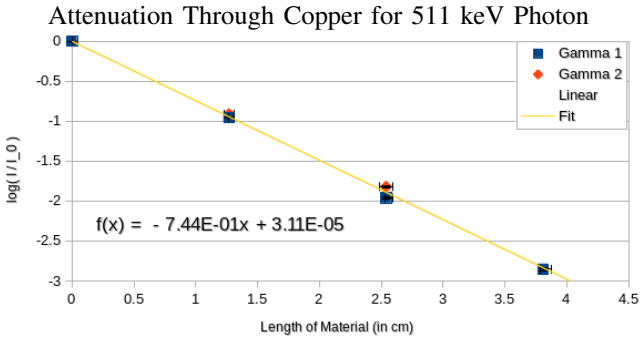

Fig. 7: The following graph shows the number of counts in their respective detector as a function of the thickness of the material in between the source and the detector. The slope tells us the attenuation coefficient of the material.

explained statistically. Therefore the 1275 keV and 511 keV photons can be considered independent of one another.

The accepted values for the attenuation coefficients for Copper are 0.7420cm^{-1} for the 511 keV photons and 0.4972cm^{-1} for the 1275 photons. The accepted values for Aluminium are 0.2260cm^{-1} for the 511 keV photons and 0.1562cm^{-1} for the 1275 keV photons[7]. Performing a least-squares linear regression on the values from Tables IV, V, VI, and VII, we

Attenuation Through Copper for 1275 keV Photon

Detector	Thickness (cm)	Intensity	$ln(I/I_0)$	ϵ
Gamma 1	0	64616	0	0.0088
	1.270	2814	-0.824	0.019
	2.540	1858	-1.239	0.023
	3.810	1046	-1.814	0.031
Gamma 2	0	3534	0	0.012
	1.270	1947	-0.596	0.023
	2.540	1127	-1.143	0.030

TABLE V: The intensity is simply the number of incidences detected by our detector. I_0 is the intensity with no material in between the source and detector. ϵ is the error in log-space as defined by Eqn. (6).

Attenuation Through Copper for 1275 keV Photon

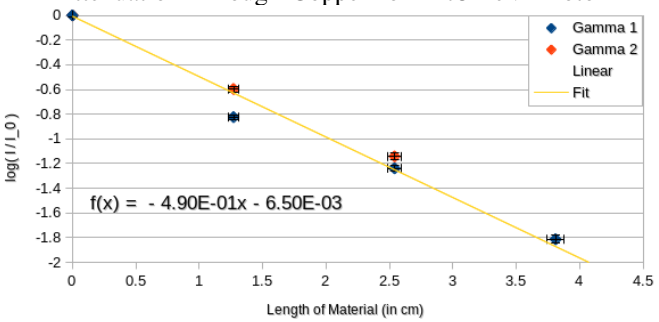

Fig. 8: The following graph shows the number of counts in their respective detector as a function of the thickness of the material in between the source and the detector. The slope tells us the attenuation coefficient of the material.

Attenuation Through Aluminium for 511 keV Photon

Detector	Thickness (cm)	Intensity	$ln(I/I_0)$	ϵ
Gamma 1	0	47634	0	0.0032
	1.270	23422	-0.7099	0.0065
	2.540	15790	-1.1042	0.0080
Gamma 2	0	26348	0	0.0044
	1.270	16469	-0.4699	0.0080
	2.540	11706	-0.8113	0.0092

TABLE VI: The intensity is simply the number of incidences detected by our detector. I_0 is the intensity with no material in between the source and detector. ϵ is the error in log-space as defined by Eqn. (6).

find the following attenuation coefficients:

$$\mu_{copper,511} = 0.7445 \pm 0.0083 cm^{-1}$$
$$\mu_{copper,1275} = 0.4896 \pm 0.0077 cm^{-1}$$
$$\mu_{aluminium,511} = 0.4053 \pm 0.0025 cm^{-1}$$
$$\mu_{aluminium,1275} = 0.1934 \pm 0.0068 cm^{-1}$$

Both of the copper attenuation coefficients are in perfect agreement with the literature values. If we only consider Gamma 2 values for the aluminium fitting, we obtain the

Attenuation Through Aluminium for 511 keV Photon

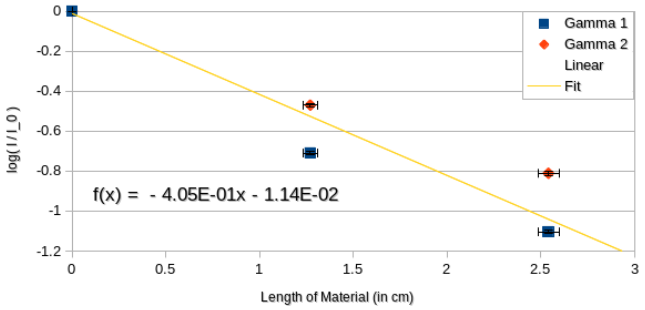

Fig. 9: The following graph shows the number of counts in their respective detector as a function of the thickness of the material in between the source and the detector. The slope tells us the attenuation coefficient of the material.

Attenuation Through Aluminium for 1275 keV Photon

Detector	Thickness (cm)	Intensity	$ln(I/I_0)$	ϵ
Gamma 1	0	6416	0	0.0088
	1.270	4424	-0.372	0.014
	2.540	3835	-0.515	0.016
Gamma 2	0	3534	0	0.011
	1.270	2866	-0.210	0.019
	2.540	2394	-0.389	0.023

TABLE VII: The intensity is simply the number of incidences detected by our detector. I_0 is the intensity with no material in between the source and detector. ϵ is the error in log-space as defined by Eqn. (6).

Attenuation Through Aluminium for 1275 keV Photon

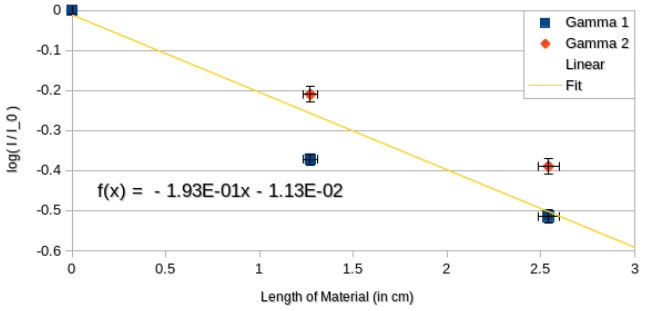

Fig. 10: The following graph shows the number of counts in their respective detector as a function of the thickness of the material in between the source and the detector. The slope tells us the attenuation coefficient of the material.

following values:

$$\mu_{aluminium,511} = 0.3291 \pm 0.0038 cm^{-1}$$
$$\mu_{aluminium,1275} = 0.1550 \pm 0.0090 cm^{-1}$$

In this case, the the 1275 keV regime perfectly agrees with the literature values. The 511 keV regime is closer though still a significant number of standard errors away.

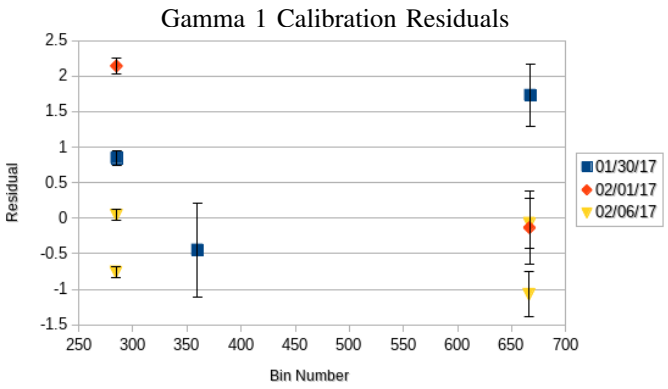

Fig. 11: The residuals are separated by the days they were observed. There does not appear to be a trend between the residuals on different days.

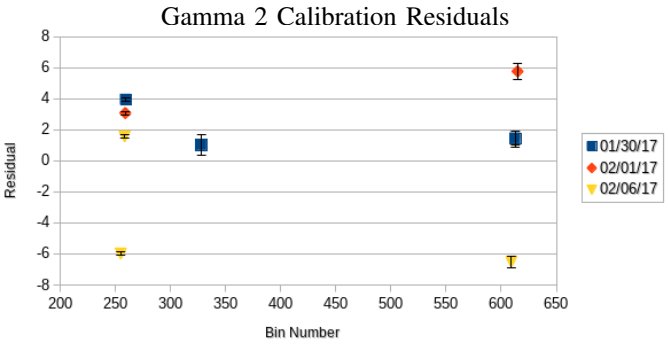

Fig. 12: The residuals are separated by the days they were observed. There does not appear to be a trend between the residuals on different days.

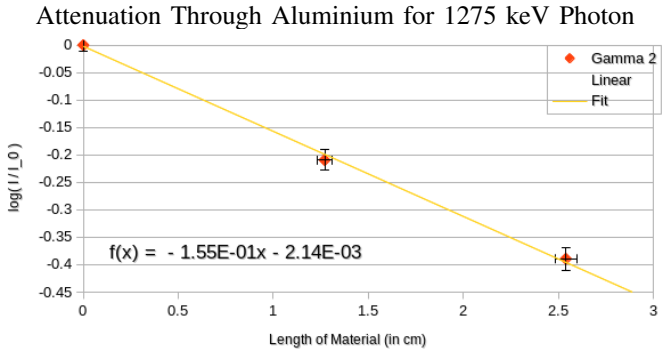

Fig. 13: The following graph shows the number of counts in only the Gamma 2 detector as a function of the thickness of the material in between the source and the detector. The slope tells us the attenuation coefficient of the material. In this instance, the data is in agreement with the literature value of 0.1562cm^{-1}[7].

V. Conclusion

Using only six runs over three different days and two different radioactive materials, we were able to approximate a rough energy calibration for both of our NaI detectors. Varying the angle of the detectors we were able to clearly show an angle dependency for the 511 keV photons while the 1275 keV coincidence rates could be explained adequately by statistical fluctuations. Out attenuation coefficient for Copper in both detectors were within one standard error of the literature values. For the Aluminium sample, we were able to achieve the literature value in one detector for one of the peak despite only having six data points all of which were taken on a single day. Given the results for Copper and small sample size, we very well might have achieved more accurate results.

VI. Acknowledgments

I would like to thank my lab partners, Brandon Coleman and Taylor Grueser, who helped with the setup, data acquisition and analysis for this report.

References

[1]"Beta-decay and gamma-ray spectroscopy with nai detectors", Introductory Laboratory – Nucleons.

[2]"Coincidence counting", E.K.A. Advanced Physics Laboratory (2002).

[3]*Nist: x-ray mass attenuation coefficients - table 1*, [Online; accessed 12-February-2017], http : / / physics . nist . gov / PhysRefData/XrayMassCoef/tab1.html.

[4]E. C. Stewart, *Harshaw scintillation phosphors, (2nd ed.)* (Harshaw Chemical Co., Cleveland, 1978).

[5]P. R. Bevington and D. K. Robinson, *Data reduction and error analysis for the physical sciences* (McGraw-Hill, 2002).

[6]A. Sonzogni, *Nudat 2*, [Online; accessed 29-January-2017], http://www.nndc.bnl.gov/nudat2/.

[7]*Nist: x-ray mass attenuation coefficients*, http://physics.nist.gov/PhysRefData/XrayMassCoef/tab3.html.